



저작자표시-비영리-변경금지 2.0 대한민국

이용자는 아래의 조건을 따르는 경우에 한하여 자유롭게

- 이 저작물을 복제, 배포, 전송, 전시, 공연 및 방송할 수 있습니다.

다음과 같은 조건을 따라야 합니다:



저작자표시. 귀하는 원저작자를 표시하여야 합니다.



비영리. 귀하는 이 저작물을 영리 목적으로 이용할 수 없습니다.



변경금지. 귀하는 이 저작물을 개작, 변형 또는 가공할 수 없습니다.

- 귀하는, 이 저작물의 재이용이나 배포의 경우, 이 저작물에 적용된 이용허락조건을 명확하게 나타내어야 합니다.
- 저작권자로부터 별도의 허가를 받으면 이러한 조건들은 적용되지 않습니다.

저작권법에 따른 이용자의 권리는 위의 내용에 의하여 영향을 받지 않습니다.

이것은 [이용허락규약\(Legal Code\)](#)을 이해하기 쉽게 요약한 것입니다.

[Disclaimer](#)

Efficiency of Uncured Monomer Removal
from Clear Aligners in Accordance with
Centrifugation Time and Temperature
in 3D-Printing Post-Processing

Ji-Eun Kim

The Graduate School
Yonsei University
Department of Dentistry

Efficiency of Uncured Monomer Removal from Clear Aligners in Accordance with Centrifugation Time and Temperature in 3D-Printing Post-Processing

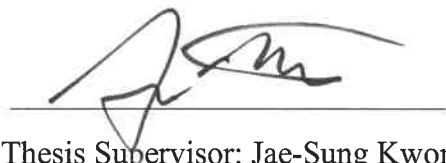
A Dissertation Thesis

Submitted to the Department of Dentistry
and the Graduate School of Yonsei University
in partial fulfillment of the
requirements for the degree of
Doctor of Dental Science

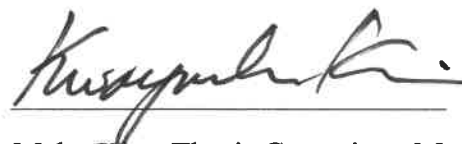
Ji-Eun Kim

June 2024

This certifies that the dissertation thesis
of 'Ji-Eun Kim' is approved.



Thesis Supervisor: Jae-Sung Kwon



Kwang-Mahn Kim: Thesis Committee Member #1



Eun-Jung Lee: Thesis Committee Member #2



Sang-Bae Lee: Thesis Committee Member #3



Utkarsh Mangal: Thesis Committee Member #4

The Graduate School
Yonsei University
June 2024

ACKNOWLEDGEMENTS

I am deeply moved to receive my doctoral degree, the pinnacle of academic achievement, here in Korea. Life doesn't always go as planned. I didn't expect to join as a teaching assistant and end up earning a Ph.D. I am sincerely grateful to *Prof. Kyoung-Nam Kim*, *Prof. Kwang-Mahn Kim*, and *Prof. Jae-Sung Kwon* for guiding me along the path of research. Meeting these professors is an incredible stroke of fortune in my life. It is also an honor to graduate alongside *Prof. Kwang-Mahn Kim*, who is retiring this year.

I would also like to extend my deepest gratitude to *Prof. Eun-Jung Lee*, *Prof. Sang-Bae Lee*, and *Prof. Utkarsh Mangal* for serving on my dissertation committee. Special thanks to *Prof. Sung-Hwan Choi*, whose insightful advice helped me complete my research.

I am also grateful to my colleagues who devoted themselves to research with me late into the night. I am especially thankful to the teaching assistants who worked with me and were understanding and considerate of my busy days with my degree. The support from everyone in the Department and Research Institute of Dental Biomaterials and Bioengineering has been immense throughout this journey.

Lastly, I extend my sincere thanks to my father *Jung-Ho Kim*, mother *Jung-Sun Park*, my younger brother *Chang-Hyun Kim*, and my eternal little cat, *Sung-Ge*, for their unwavering love and support. I also appreciate the encouragement from my relatives and friends who cheered me on from afar. Your constant encouragement has brought me to where I am today.

I will continue to strive for growth and development, always remembering to be grateful.

Ji-Eun Kim

TABLE OF CONTENTS

LIST OF FIGURES	iv
LIST OF TABLES	vi
ABSTRACT	vii
I. INTRODUCTION	1
1. 3D-printed clear aligner	1
2. Post-processing stage in 3D-printing	4
3. Centrifugal cleaning method in 3D-printing	5
4. Research objective and null hypothesis	7
II. MATERIALS AND METHODS	8
1. Rheological analysis of 3D printing resin	8
2. Specimens preparation	9
3. Weight of aligners after post-curing	13
4. Measurement of optical properties	14

4.1. Transmittance with UV-visible spectrophotometer (UV-vis)	14
4.2. Visual observation	15
5. Surface analysis with scanning electron microscopy (SEM)	16
6. Assessment of clear aligner geometry	17
7. Stress relaxation test.....	18
8. Cytotoxicity analysis	20
8.1. Cell culture	20
8.2. Cytotoxicity evaluation of extracts	21
9. Statistical analysis	22
 III. RESULTS	 23
1. Results of rheological analysis of 3D printing resin	23
2. Weight of aligners after post-curing	24
3. Optical properties.....	25
3.1. Transmittance with UV-visible spectrophotometer (UV-vis)	25
3.2. Visual observation	27
4. SEM surface morphology.....	28
5. Relative assessment of clear aligner geometry	30
6. Results of stress relaxation	33

7. Cytotoxicity analysis	34
IV. DISCUSSION	36
V. CONCLUSION	42
REFERENCES	44
ABSTRACT (in Korean)	47

LIST OF FIGURES

Figure 1. Stages of laboratory procedure in the manufacturing of direct 3D-printed clear aligner.....	3
Figure 2. Schematic diagram of the flowability experiment of solutions stored at each temperature. RT; Room temperature, HT; High temperature.....	8
Figure 3. Flowchart describing the study design and experiment workflow. NT; Not treated, IPA; Isopropyl alcohol, RT; Room temperature, HT; High temperature	11
Figure 4. STL image of the printed clear aligner and schematic diagram of the centrifuge chamber with temperature control function	12
Figure 5. Schematic diagram of stress relaxation test (blue dots indicates cylindrical shape printed with the specimen, blue lines indicate measured distance); (A) Initial intermolar width (IM), (B) IM measured immediately after the clear aligner was bent and placed into the mold (0 mins)	19
Figure 6. Results of viscosity. RT; Room temperature, HT; High temperature.....	23
Figure 7. Weight graph of 3D-printed clear aligner with support removed according to cleaning method. (Different lowercase letters indicate significant differences in the average between groups ($p < 0.05$)). NT; Not treated, IPA; Isopropyl alcohol, RT; Room temperature, HT; High temperature.....	24
Figure 8. Transmittance curves of all groups of clear aligners with SD. NT; Not treated, IPA; Isopropyl alcohol, RT; Room temperature, HT; High temperature	25
Figure 9. Comparison of translucency on gray and white backgrounds by cropping the right maxillary central incisor region from each group's specimens: (A) schematic diagram, (B) IPA, (C) NT, (D) RT-2, 4, 6 and (E) HT-2, 4, 6. NT; Not treated,	

IPA; Isopropyl alcohol, RT; Room temperature, HT; High temperature 27

Figure 10. SEM image of clear aligners: (A) A schematic diagram of the SEM image capture locations, (B) IPA, (C) NT, (D) RT-2, 4, 6 and (E) HT-2, 4, 6. NT; Not treated, IPA; Isopropyl alcohol, RT; Room temperature, HT; High temperature 29

Figure 11. Comparison of color difference maps of anterior region evaluated by using *Geomagic* software program: (A) A schematic diagram illustrating the residual monomer pattern on the printed clear aligner before the cleaning process; (B) NT; (C) RT-2, 4, 6; (D) HT-2, 4, 6. NT; Not treated, RT; Room temperature, HT; High temperature 31

Figure 12. Cell viability of clear aligner model for each experimental group compared to the blank (B). The yellow line represents the minimum ISO standard (ISO 10993-5, 2009) criterion: a cell viability less than 70 % is considered cytotoxic. When lowercase letters above the bar graph are the same, it signifies that there are no significant differences between the groups ($p < 0.05$). Conversely, differing lowercase letters indicate significant differences between the groups ($p < 0.05$). NC; negative control, PC; positive control, NT; Not treated, IPA; Isopropyl alcohol, RT; Room temperature, HT; High temperature 35

LIST OF TABLES

Table 1. The experimental group codes according to the cleaning method.....	10
Table 2. Relative transmittance (%) calculated from the area under the curve measured by UV-vis spectrophotometry.....	26
Table 3. The accuracy of seven groups for anterior expressed in root mean square with SD (μm).....	32
Table 4. Shape recovery ratio of clear aligners specimens (%).....	33

ABSTRACT

Efficiency of Uncured Monomer Removal from Clear Aligners in Accordance with Centrifugation Time and Temperature in 3D-Printing Post-Processing

Ji-Eun Kim

Department of Dentistry

The Graduate School, Yonsei University

(Directed by Professor Jae-Sung Kwon, M.D., Ph.D.)

The advancement of three-dimensional (3D)-printing technology has enabled the direct production of customized clear aligners from transparent resin materials based on dental computer-aided design. To manufacture 3D-printed clear aligners, the patient's dentition is 3D-scanned, target models for each orthodontic stage are designed, and then printed. After printing, the aligners are separated from the platform and undergo a series of post-processing steps, among which the cleaning stage for removing uncured monomers is crucial for accurate fabrication and achieving appropriate physical properties.

With the drawbacks of the conventional chemical cleaning method using isopropyl

alcohol (IPA) being highlighted, the non-chemical centrifugal cleaning method has recently gained attention. This study investigated the influence of time and temperature of the centrifugal cleaning method on the removal of uncured monomers from 3D-printed clear aligners.

The cleaning temperature was controlled using a heating wire installed inside the centrifuge. The 3D-printed clear aligners were cleaned with IPA or centrifuge (g-force 27.95 g) cleaning 2, 4, and 6 mins at 23 ± 2 °C (RT) or 55 ± 2 °C (HT) respectively, and rheological analysis, weight measurement, transparency evaluation, surface analysis, 3D data comparison, stress relaxation characteristics, and cytotoxicity evaluation were performed to evaluate the effect.

The results showed that viscosity decreased by 2.34 times at HT compared to RT, and the weight of clear aligners decreased with increasing centrifugation cleaning time and temperature ($p < 0.05$). The transmittance value measured by UV-vis spectrophotometer to determine transparency was highest in the NT group, and the transmittance value tended to decrease as temperature and washing time increased. The IPA group showed significantly lower transparency than other groups ($p < 0.05$). However, when visually observing the transparency of clear aligner specimens, there was no difference between groups except for the IPA group. Scanning electron microscopy revealed that the surface of the IPA group was the roughest. Internal fit evaluation through 3D scanning of plaster models showed that the centrifugation groups exhibited relatively good precision. The non-treated group had a high Root Mean Square value ($p < 0.05$) and showed positive (+) deviations in the incisal region. Stress relaxation tests showed that the shape of the aligners recovered over time, with all groups exhibiting over 95 % recovery after 60 minutes, and there was no significant difference based on the cleaning method ($p < 0.05$). Cytotoxicity results showed that all groups met the ISO standard criteria.

In conclusion, while there were significant differences in uncured monomer removal efficiency and some physical properties depending on time and temperature, there was no

substantial impact on cytotoxicity and stress relaxation behavior. Notably, centrifugal cleaning at HT for 2 minutes effectively removed uncured monomers while maintaining the physical properties (weight, transparency, surface characteristics, dimensional stability and shape recovery ratio) of clear aligners. Therefore, centrifugation at HT for 2 minutes is considered an appropriate clinical cleaning method that minimizes working time and effectively removes uncured monomers without significantly affecting the physical properties of clear aligners.

Key words: Centrifugation, Clear aligner, 3D-printing, Post-processing, Centrifugal cleaning, Time, Temperature

**Efficiency of Uncured Monomer Removal
from Clear Aligners in Accordance with
Centrifugation Time and Temperature
in 3D-Printing Post-Processing**

Ji-Eun Kim

Department of Dentistry

The Graduate School, Yonsei University

(Directed by Professor Jae-Sung Kwon, M.D., Ph.D.)

I. INTRODUCTION

1. 3D-printed clear aligner

The core principle of orthodontic therapy involves making slight adjustments to teeth positioning using a sequence of custom-made, transparent aligners (Kesling, 1945). Orthodontic devices must have appropriate biocompatibility, mechanical properties and durability to realize tooth movement.

Orthodontic treatment that can satisfy the aesthetic needs of patients is clear aligner

treatment, which is used thanks to the advancement of Computer-Aided Design/Computer-Aided Manufacturing (CAD/CAM) technology. The preferred method for creating these clear aligners has been to use thermoplastic materials, which are heated and then formed over 3D-printed treatment stage models (Rajasekaran and Chaudhari, 2023). However, challenges such as limited options for appliance customization, inconsistent quality among thermoplastic sheets, and less predictable treatment outcomes have been noted (Bichu et al., 2023). Additionally, the single-use 3D-printed models that simulate the treatment stage for clear aligner production contribute to environmental concerns adding to the generated material waste (Bichu et al., 2023; Caelli et al., 2023; Lee et al., 2022).

A recent advancement to address the challenges previously outlined involves directly 3D-printing the clear aligners from CAD designs using clear resin materials (Koenig et al., 2022). The 3D-printing process follows the core principles of additive manufacturing for resin-based appliances and using vat-polymerization and consists of three main phases: 3D scanning of the teeth, the additive printing process itself, and post-processing steps (Figure 1). This approach eliminates the necessity of producing an intermediate model, thus conserving time and labor, and enables precise customization of the clear aligner dimensions to meet the specific anatomical needs of each patient. Additionally, it significantly diminishes the reliance on single-use polymeric treatment models (Vasamsetty et al., 2020).

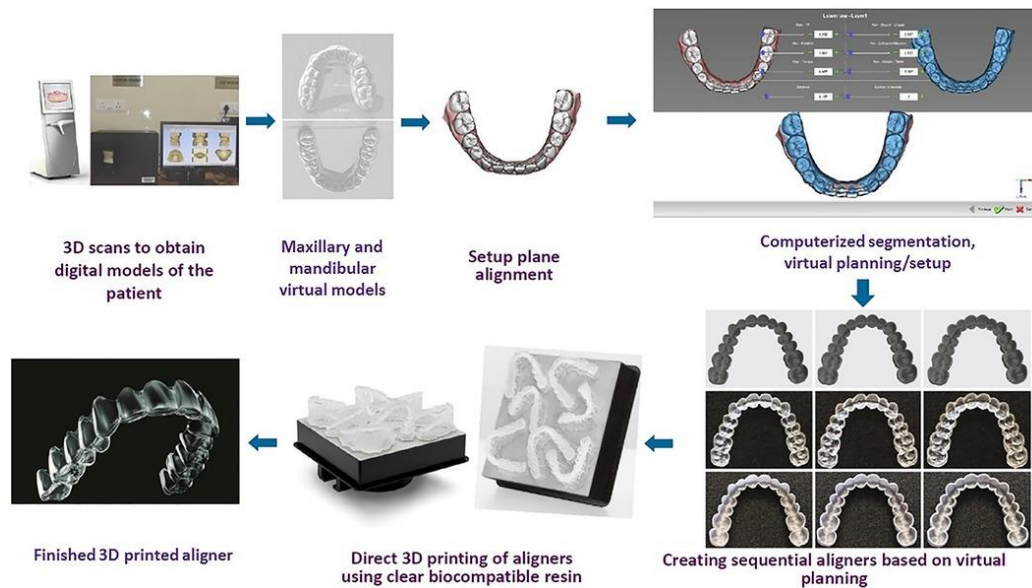


Figure 1. Stages of laboratory procedure in the manufacturing of direct 3D-printed clear aligner (Rajasekaran and Chaudhari, 2023).

2. Post-processing stage in 3D-printing

The current post processing in 3D-printing consists of following three-stage; removing the supporter, cleaning, and post-curing after printing. The cleaning stage, which is manual, entails the removal of any uncured monomer and ensuring the aligner's durability and safety through post-curing (Jang et al., 2021). This stage is essential because the surfaces of appliances immediately after 3D-printing often have excess uncured monomer, making cleaning a critical step for biological safety. Most manufacturers recommend using an activated bath of organic solvents, such as ethanol or isopropyl alcohol (IPA), to clean the surfaces of 3D-printed appliances (Lambart et al., 2022; Reymus et al., 2020). However, solvents that possess high volatility and flammability can lead to significant increases in airborne particles and total volatile organic compounds (TVOC) during the cleaning process (Bowers et al., 2022). In addition, the chemical effects of these solvents on acrylic-based polymers can result in a reduction of translucency of clear resin material (Park et al., 2023). In addition, organic solvent can potentially exert unpredictably alter the surface physical properties (Lambart et al., 2022). Therefore, with the sub-millimeter dimensional characteristic of the clear aligner, cleaning method could potentially have major influence on treatment outcome. Hence, exploring non-chemical cleaning methods, such as centrifugation, for the removal of residual monomers has been recently proposed for 3D-printed clear aligners.

3. Centrifugal cleaning method in 3D-printing

The technique of separating substances under the influence of centrifugal force is termed as centrifugation. A centrifuge is a machine that rotates around a fixed axis, consisting of components such as the centrifuge chamber, motor, rotor, tub, and safety lid. During operation, the force acts perpendicularly to the axis of rotation, that is, in an outward direction. When an object moves in a circular motion having a constant or steady angular velocity, it experiences an outward force, F (Centripetal acceleration).

$$F = \omega^2 r$$

where,

ω is the angular velocity in radians,

r is the radius of rotation (cm).

Rotations per minute (rpm) is used to express these relationships. The speed at which a centrifuge operates is given in terms of rpm. Rpm can be converted to radians using the formula.

$$\omega = \frac{2\pi}{60} \cdot \text{rpm}$$

Recently, to minimize air pollution that may occur during 3D printing (Ryan and Hubbard, 2016), centrifugation, non-chemical cleaning method, is widely used in dentistry as a method to remove residual monomers remaining on 3D-printed objects during the printing process before final photocuring. In the dental world, the centrifugation cleaning method is used for or in the production of 3D-printed temporary prosthesis and clear aligner, depending on the manufacturer's suggestion (Mayer et al., 2021).

The effectiveness of centrifuge monomer removal can be influenced by factors such as the weight of the object, rotational speed, distance from the rotation axis to the object (Dong, 2020), rotation time, viscosity, and others (Gandhi et al., 2022). Although previous studies have explored similar solvent free centrifugation method, the process has

been largely empirical with minimal explanation of the key parameters (Grant et al., 2023; Mayer et al., 2021). Therefore, it is necessary to investigate the effect of variables on the cleaning effect using centrifugation.

4. Research objective and null hypothesis

The objective of this study was to investigate the optimal centrifugation cleaning time and temperature conditions in the post-processing cleaning stage of 3D-printing to effectively remove uncured monomers while maintaining the physical properties (including weight, transparency, internal surface morphology, stress relaxation characteristics) and cytotoxicity of clear aligners.

Herein, it was null hypothesized that increasing time and temperature in centrifugal cleaning would not influence the weight, optical transparency, internal surface morphology, stress relaxation and cytotoxicity of the 3D-printed clear aligners.

II. MATERIALS AND METHODS

1. Rheological analysis of 3D printing resin

Flowability and viscosity were measured to evaluate the flow properties of 3D-printing resin at 23 ± 2 °C (room temperature; RT) and 55 ± 2 °C (high temperature; HT). For flowability, the resin solution was stored at RT and HT for 5 minutes each, and then 80 μ L of the solution was dropped onto a glass slide, and flowed tilted 45° for 15 seconds to check the difference in flowability between the two temperatures (n=5) (Figure 2).

Viscosity tests were performed using an MCR 702e dynamic shear rheometer (Anton Paar, GmbH, Gratz, Austria) equipped with diameter 25 mm parallel plates. The gap between bottom plate and spindle plate was set to 1 mm. Resin viscosity was also measured at temperatures RT and HT, with a shear rate range of 0.1 to 100 s^{-1} .

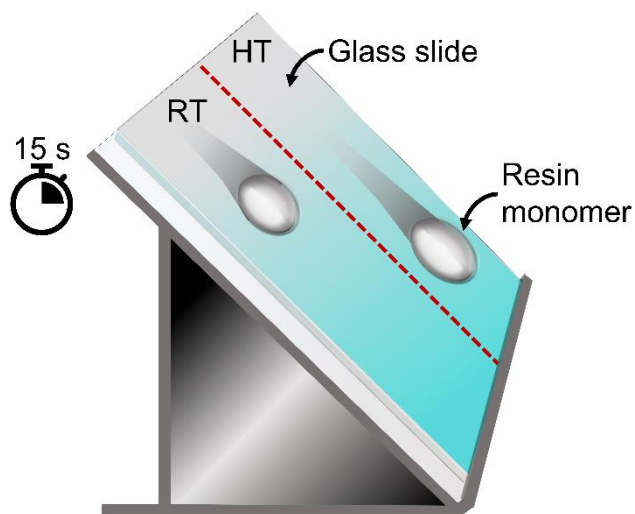


Figure 2. Schematic diagram of the flowability experiment of solutions stored at each temperature. RT; Room temperature, HT; High temperature.

2. Specimens preparation

The study workflow is as shown in Figure 3. A typodont model representing maxillary dental arch (Dentiform; Nissan Dental Products, Kyoto, Japan) was used and scanned using an intraoral scanner (Medit i600, Medit Corp., Seoul, Korea) to create an standard tessellation language (STL) file (standard data). Next, supports were added, and the aligners were designed with a predetermined thickness of 0.5 mm and an offset of 50 μ m. The orientation of the models was set with the posterior section facing the platform at a 45° angle. They were then printed on the platform using an LCD 3D-printer (UNIZ NBEE, UNIZ Technology LLC, USA) with 49.8 μ m XY resolution using a photo-polymerizable polyurethane resin (Tera Harz TC-85, Graphy Inc., Seoul, Korea).

After 3D-printing, the clear aligners were separated from the build platform and two different cleaning methods, IPA and centrifugal cleaning, were used to remove uncured monomer from the 3D-printed clear aligner: IPA group (negative control), the clear aligners were immersed in isopropyl alcohol (Sigma-Aldrich, 99.5 %) and ultrasonic rinsed for 1 minute using an ultrasonic cleaner (Sae Han Ultrasonic Co., Korea), and the clear aligners were placed on paper towels in the hood chamber to air dry for 5 mins. The centrifugation group were treated using a centrifuge machine (MR-H100WM, Viska, Germany) with a heating element (YD07005-12002A, WOOHEATER Co., LTD, Korea) installed on the outside of the tub (Figure 4).

The temperature was controlled at 23 ± 2 °C (room temperature; RT) and 55 ± 2 °C (high temperature; HT). The HT setting used a temperature controller (OKE-6428HC, Sewon, Korea) and centrifugation (g-force 27.95 g) was performed at 500 rpm for 2, 4, and 6 minutes at each temperature, respectively. The group that did not undergo any treatment is called NT (not treated) (Table 1). The supports were then removed from the clear aligners, and a 20 minutes curing process was performed under nitrogen using the Tera Harz Cure THC 2 UV curing system (Graphy, Seoul, Korea).

Table 1. The experimental group codes according to the cleaning method

Group code	Cleaning Method
NT	Not treated
IPA	IPA; 23 ± 2 °C, ultrasonic 1 min
RT-2	Centrifugation; 23 ± 2 °C, 2 mins
RT-4	Centrifugation; 23 ± 2 °C, 4 mins
RT-6	Centrifugation; 23 ± 2 °C, 6 mins
HT-2	Centrifugation; 55 ± 2 °C, 2 mins
HT-4	Centrifugation; 55 ± 2 °C, 4 mins
HT-6	Centrifugation; 55 ± 2 °C, 6 mins

NT; Not treated, IPA; Isopropyl alcohol, RT; Room temperature, HT; High temperature.

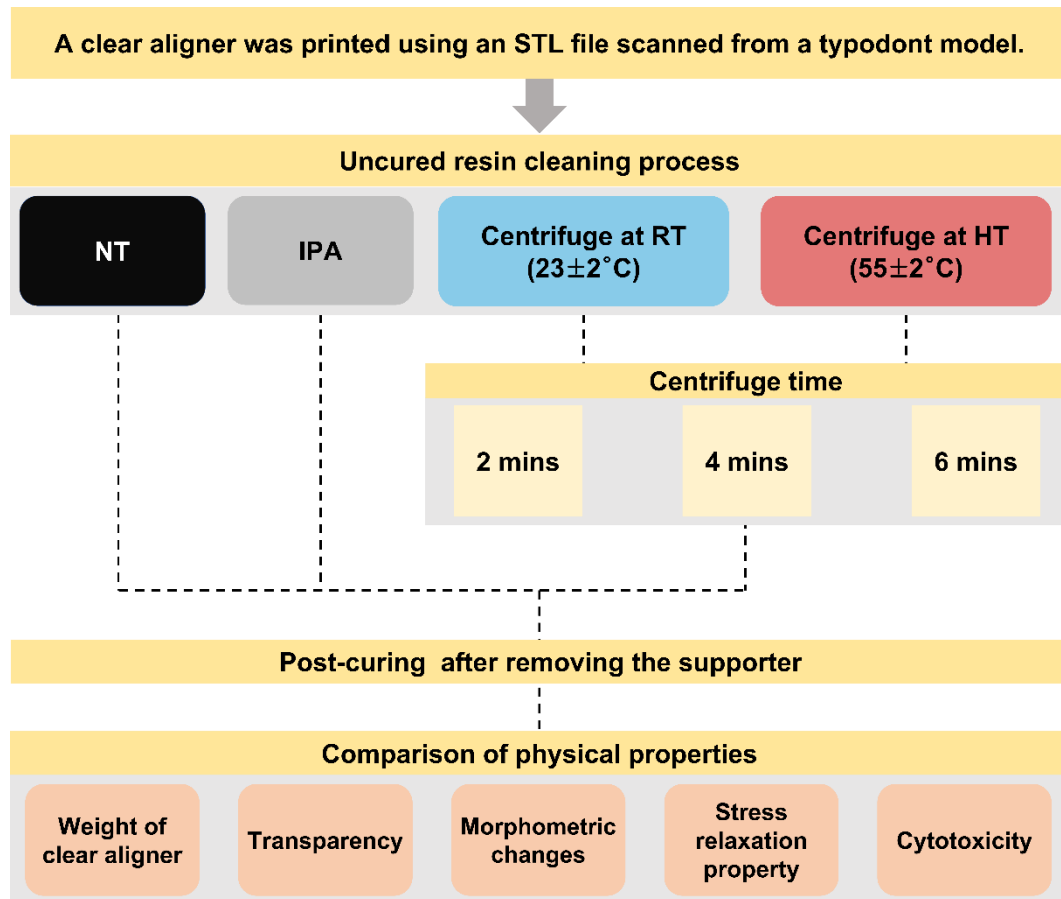


Figure 3. Flowchart describing the study design and experiment workflow. NT; Not treated, IPA; Isopropyl alcohol, RT; Room temperature, HT; High temperature.

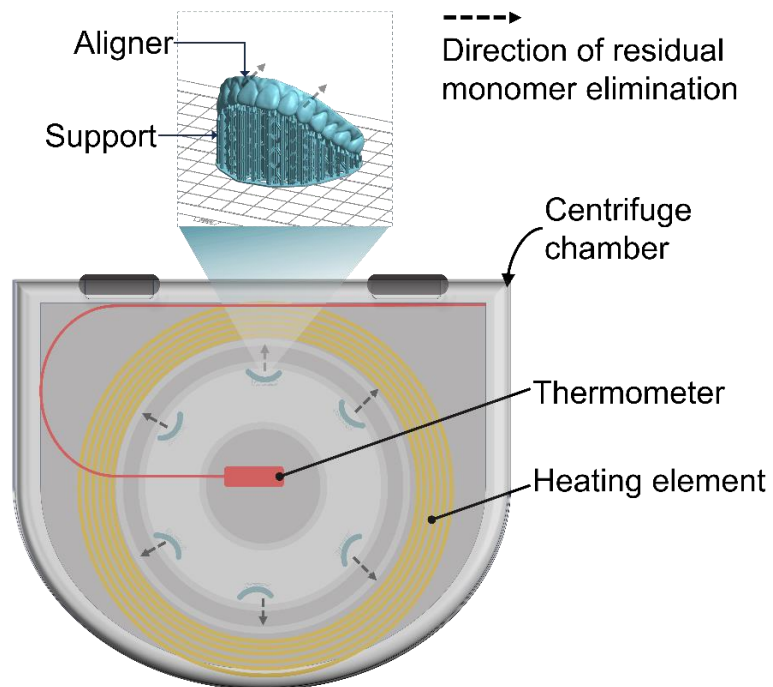


Figure 4. STL image of the printed clear aligner and schematic diagram of the centrifuge chamber with temperature control function.

3. Weight of aligners after post-curing

After printing the clear aligner specimen, post-processing was performed for each group (n=5) according to each condition. Next, the supports were carefully removed, and the clear aligners underwent post-curing. The weight of each manufactured model was then measured using a precision analytical balance (Metler Toledo ML104, Switzerland) which is accurate to ± 0.1 mg. To minimize contamination during the support removal process and ensure consistent handling practices, fresh latex gloves were worn for each procedure.

4. Measurement of optical properties

4.1. Transmittance with UV-visible spectrophotometer (UV-vis)

The labial portion of the central incisor of clear aligner was positioned horizontally in front of the sample holder of a UV-visible spectrophotometer (Jasco UV-vis V-630, Tokyo, Japan) and aligned with the halogen lamp light source. Transmittance was measured in transmission mode for each sample. Transparency measurements for each sample (n=3) were performed in the wavelength range of 400-700 nm. Each specimen was assessed with three consecutive measurements using the spectrophotometer, and the average value were calculated. The results were presented as area value (%) under the curve for each group computed using software (OriginLab, OriginPro 8.5, USA) for transparency comparison (Youm et al., 2024). The area value (%) was computed using the following formula:

$$\frac{\int_{400}^{700} |t(x)| dx (\%nm)}{\int_{400}^{700} |t'(x)| dx (\%nm)} \times 100 = Translucency(\%)$$

where,

$t(x)$: light intensity of each spectrum through the specimen,

$t'(x)$: light intensity of each spectrum of the light source without any sample.

4.2. visual observation

To visually compare the change in transparency the labial portion of the right central incisor from the clear aligner was isolated and photographed using a smartphone (Galaxy Z Flip3 5G, SM-F711N; Samsung Electronics Co., Ltd., Seoul, South Korea) against two contrasting backgrounds: a gray background with an RGB value of (191, 191, 191) and a white background with an RGB value of (255, 255, 255). The photographs were taken under common fluorescent lighting in an indoor environment. The smartphone's main camera, which features a 26 mm focal length and an f/1.8 aperture, was used to capture the images. The photographs were taken at ISO 80, with a shutter speed of 1/120 s and an exposure compensation of 0.0 exposure value.

5. Surface analysis with scanning electron microscopy (SEM)

A representative specimen from each group was observed under a SEM (JEOL JSM-IT-500HR, Tokyo, Japan) focusing on the region of interest (ROI) at the cervical 1/3 portion of the aligner. Before the SEM analysis, the specimen was platinum sputter coated for 90 s in a coating machine. The SEM micrographs were obtained at a magnification of $\times 100$ in a vacuum condition, and an accelerating voltage of 15.0 kV.

6. Assessment of clear aligner geometry

The plaster models were created by pouring gypsum (Mg Crystal Rock, Maruishi Gypsum Co. LTD., Osaka, Japan) into the support-attached printing models. Before the 3D superimposition, the cast models were scanned using a Model Scanner (Medit i600, Medit Corp., Seoul, Korea) to obtain 3D data for each experimental group (n=3). The acquired scan data was saved in STL format and precision comparative assessment was conducted using a 3D morphometric program (Geomagic GmbH, Stuttgart, Germany) in the anterior region from canine. Scanned data of the cast model (reference data) was overlaid with the standard data. After initial automatic alignment, the data sets were optimally aligned using Best Fit alignment, and the deviation for each specimen was calculated as the root mean square (RMS) value. The RMS value was computed using the following formula:

$$RMS = \frac{\sqrt{\sum_{i=1}^n (X_{1,i} - X_{2,i})^2}}{\sqrt{n}}$$

where,

$X_{1,i}$ is measured points from the Reference CAD data;

$X_{2,i}$ is measured data from the specimen's scan data;

n is total number of measurement points

7. Stress relaxation test

For the stress relaxation test, specimens (n=5) were printed with cylindrical shapes (diameter: 0.7 mm, height: 0.5 mm) attached to both mesiobuccal cusp tips of the clear aligner. The initial intermolar width (IM), which is the distance between the cusp tips of the right and left first molar (Figure 5A), was measured in millimeters. Afterwards, the clear aligner of each group was immersed in distilled water (DW) at 80 °C (Lee et al., 2022), which is higher than the transition temperature (T_g) of 3D-print resin used in this study, for 1 minute to make the specimen moldable. The specimens were bent in half at RT and placed in a mold (35 mm in width and 68 mm in length) (Figure 5B). The IM was immediately measured and recorded as 0 minutes, and the specimens were maintained in this position for 5 minutes. Afterward, the specimens were immersed in a water bath at 37 °C, and the stress relaxation phenomenon of the specimens was recorded at 10, 30, and 60 minutes.

$$\text{Shape recovery ratio} = \frac{IM}{\text{initial IM}} \times 100 \%$$

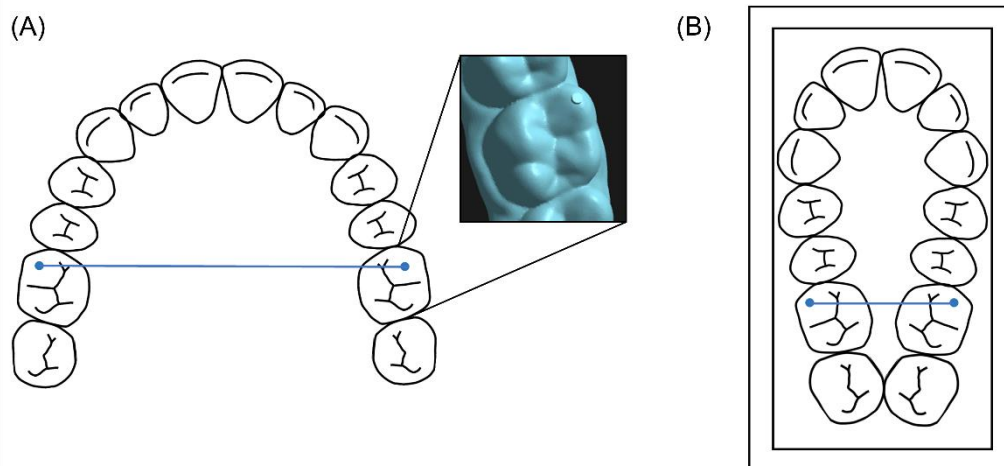


Figure 5. Schematic diagram of stress relaxation test (blue dots indicates cylindrical shape printed with the specimen, blue lines indicate measured distance); (A) Initial intermolar width (IM), (B) IM measured immediately after the clear aligner was bent and placed into the mold (0 mins).

8. Cytotoxicity analysis

8.1. Cell culture

Subcutaneous connective tissue-derived mouse fibroblast cell line L929 was used for the investigation. The L929 cells were cultured in RPMI 1640 cell culture medium (Welgene, Gyeongsangbuk-do, Korea), supplemented with 1 % antibiotic-antimycotic (Gibco, Grand Island, NY, USA) and 10 % fetal bovine serum (FBS; Gibco, Grand Island, NY, USA).

The culture medium was replenished every 2 - 3 days, maintaining a constant incubation temperature of 37 °C and a humidified atmosphere with 5 % CO₂. Adherent L929 cells were harvested as follows: first, cells were detached using 0.05 % trypsin-EDTA (Gibco, Grand Island, NY, USA); then, centrifugation was performed at 1200 rpm for 3 min, followed by resuspension in the culture medium. Subsequently, cell counts were determined providing results in terms of live/dead cell numbers per mL.

8.2. Cytotoxicity evaluation of extracts

The cytotoxicity evaluation followed the procedures outlined in ISO 10993-5 (ISO, 2009) and ISO 10993-12 (ISO, 2012). To prepare extracts, specimens of clear aligner were soaked in RPMI 1640 culture medium for 24 h at 37 °C, maintaining a ratio of 0.2 g/mL (sample weight/culture medium volume). RPMI 1640 eluted for 24 hours was utilized as the blank group for control purposes, while 0.1 % phenol solution served as the positive control, and a polyethylene (PE) film was used as the negative control.

L929 cells were seeded in a 96-well plate at a density of 1×10^4 cells per well and incubated in RPMI 1640 for 24 h at 37 °C with 5 % CO₂. Subsequently, the L929 cells were exposed to the extracted liquid from each sample at a concentration of 100 % for an additional 24 h after removing the medium. The extracted liquid was then removed, and the cytotoxicity assessment of clear aligner specimen was carried out using the methylthiazole tetrazolium (MTT) assay, comparing the results with the blank group.

For the MTT assay, a freshly prepared MTT solution was used, consisting of thiazolyl blue tetrazolium bromide (MTT; Sigma-Aldrich, St. Louis, MO, USA) dissolved in phenol red-free RPMI 1640 medium at a concentration of 1 mg/mL. This solution was filtered through a syringe and syringe filter with a pore size of 0.20 µm (DISMIC-25CS, ADVANTEC, Tokyo, Japan). In each well, 50 µL of MTT solution was added, and the plates were subsequently incubated in a 37 °C incubator with 5 % CO₂ for 2 hours. After incubation, the MTT solution was replaced with 100 µL of dimethyl sulfoxide (Sigma-Aldrich, St. Louis, MO, USA) to dissolve the formazan product. The absorbance was measured using a Microplate Spectrophotometer (Epoch, Bio Tek, Winooski, VT, USA) at 570 nm. Cell viability was calculated as the percentage of optical density (OD) relative to the blank (set at 100 %).

9. Statistical analysis

Statistical analysis was performed by using statistical software (IBM SPSS Statistics v27.0; IBM Corp., Armonk, NY). The non-parametric Kruskal-Wallis test was performed to compare differences in the weight, UV-vis transmittance, cytotoxicity and mean RMS values of the clear aligners, after which Mann-Whitney U tests were conducted for multiple comparisons. Results of stress relaxation test was performed using two-way ANOVA.

III. RESULTS

1. Results of rheological analysis of 3D printing resin

To measure flowability, the resin solution that flowing down from the slide glass for 15 seconds was measured to be 16.26 ± 1.14 mm at RT and 38.14 ± 3.56 mm at HT. Resin viscosity at each temperature is shown in Figure 6. The RT value was higher than the HT value in the shear rate range of 0.1 to 100 s^{-1} .

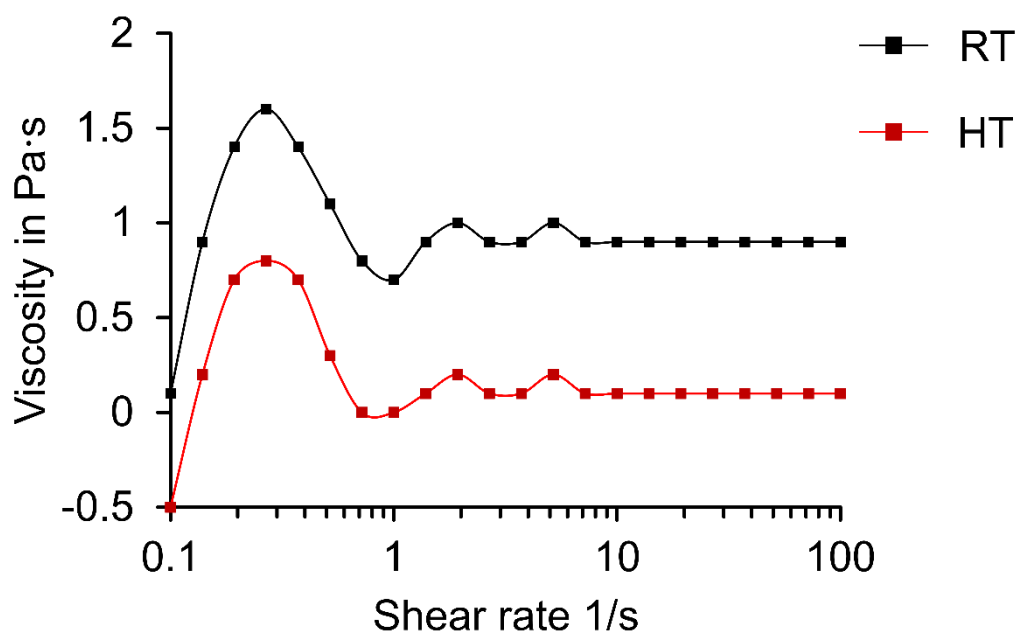


Figure 6. Results of viscosity. RT; Room temperature, HT; High temperature.

2. Weight of aligners after post-curing

There was a significant difference in weight between the eight groups ($p < 0.05$). The final specimen weights for groups NT (2.47 ± 0.04 g), IPA (1.73 ± 0.03 g), RT-2 (2.23 ± 0.01 g), RT-4 (2.18 ± 0.07 g), RT-6 (2.19 ± 0.05 g), HT-2 (2.18 ± 0.01 g), HT-4 (2.14 ± 0.02 g), and HT-6 (2.15 ± 0.02 g). The average weight was significantly higher in the NT group and significantly lower in the IPA group compared to the other groups ($p < 0.05$). There was a significant difference in weight depending on time and temperature, but there was no significant difference between RT-4, 6 and HT-2, and between HT-4 and 6 ($p > 0.05$) (Figure 7).

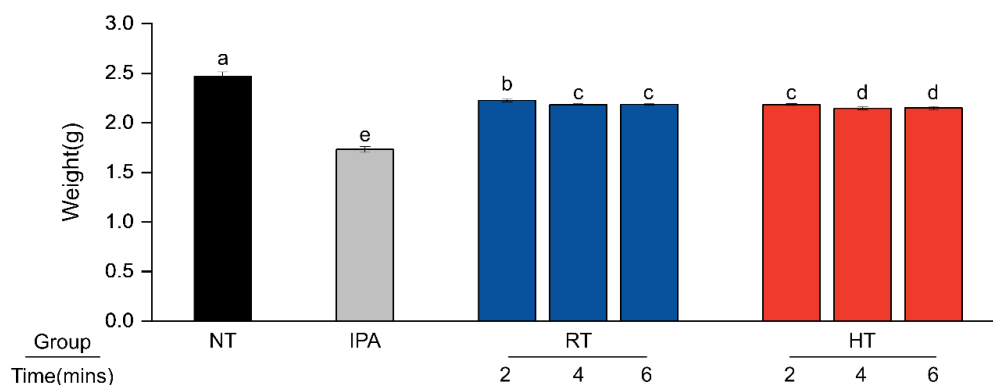


Figure 7. Weight graph of 3D-printed clear aligner with support removed according to cleaning method. (Different lowercase letters indicate significant differences in the average between groups ($p < 0.05$)). NT; Not treated, IPA; Isopropyl alcohol, RT; Room temperature, HT; High temperature.

3. Optical properties

3.1. Transmittance with UV-visible spectrophotometer (UV-vis)

The calculated areas under the transmittance curves (Figure 8) for each cleaning method presented transmittance (%) in descending order: NT, RT-2, RT-4, RT-6, HT-2, HT-4, HT-6, IPA, as shown in Table 2. RT exhibited higher transmittance compared to HT, with RT-2, RT-4, and RT-6 showing consistently higher values than their HT counterparts. Transparency tended to decrease with increasing centrifugation time within both the RT and HT groups.

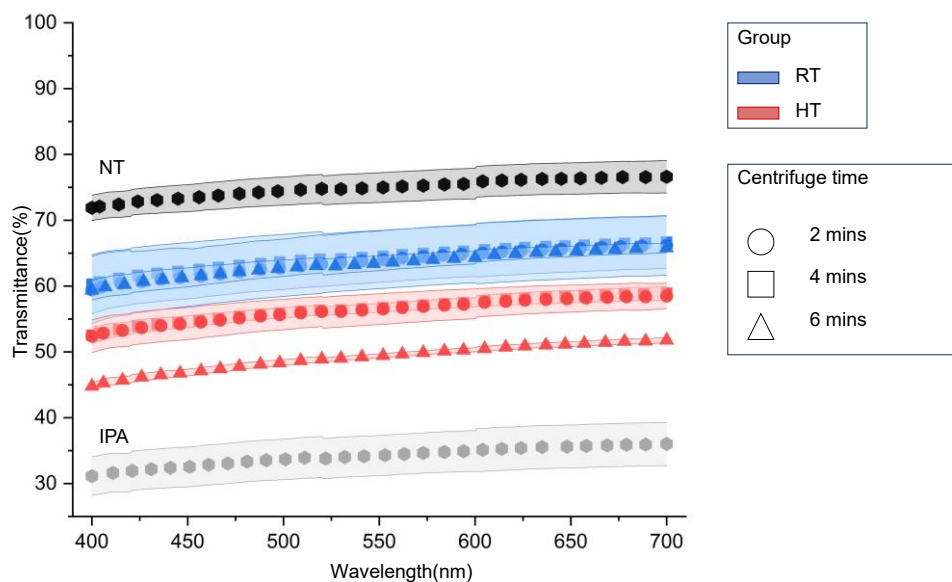


Figure 8. Transmittance curves of all groups of clear aligners with SD. NT; Not treated, IPA; Isopropyl alcohol, RT; Room temperature, HT; High temperature.

Table 2. Relative transmittance (%) calculated from the area under the curve measured by UV-vis spectrophotometry

Group	NT	IPA	RT-2	RT-4	RT-6	HT-2	HT-4	HT-6
Mean	74.89 ^a	34.16 ^b	64.31 ^a	63.65 ^a	63.36 ^a	56.55 ^a	56.30 ^a	49.14 ^a
± SD	2.22	3.12	4.08	4.50	1.10	0.82	2.26	0.38

Different lowercase letters indicate significant differences in the average between groups ($p < 0.05$). NT; Not treated, IPA; Isopropyl alcohol, RT; Room temperature, HT; High temperature.

3.2. Visual observation

In visual observation, comparing transparency in the two contrasts background (Figure 9A), IPA showed hazy dull appearance compared to other groups (Figure 9B). There were no differences found between the NT (Figure 9C), RT (Figure 9D) and HT (Figure 9E) groups.

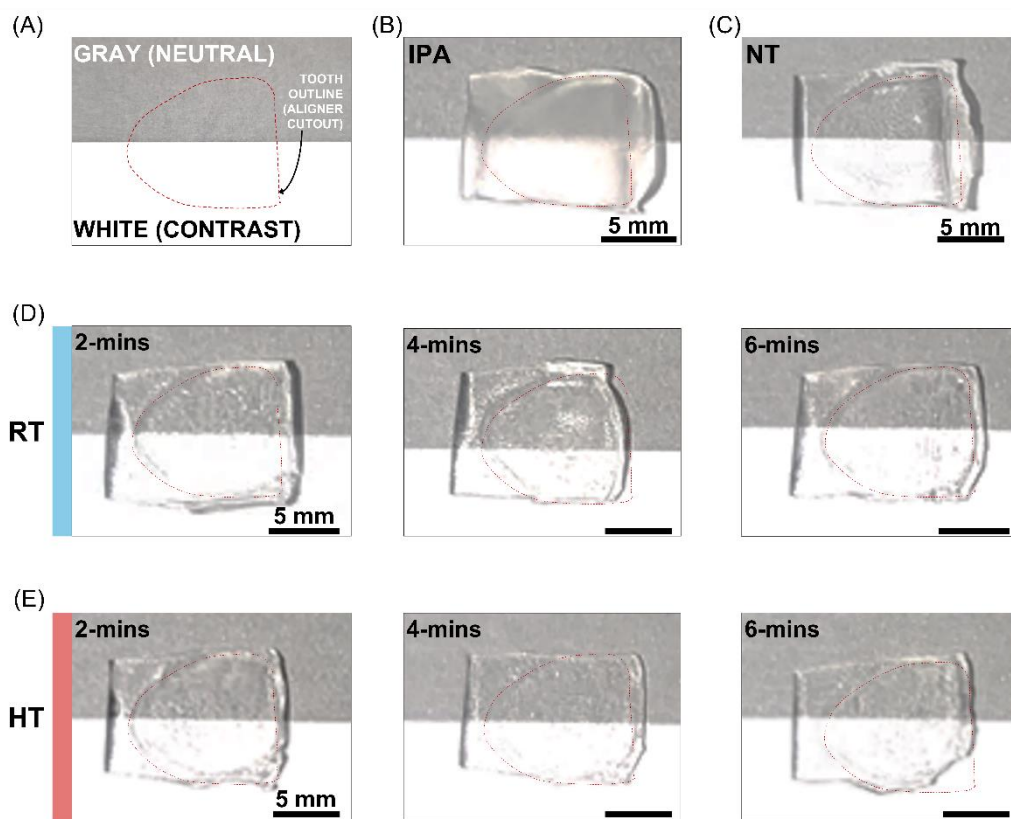


Figure 9. Comparison of translucency on gray and white backgrounds by cropping the right maxillary central incisor region from each group's specimens: (A) schematic diagram, (B) IPA, (C) NT, (D) RT-2, 4, 6 and (E) HT-2, 4, 6. NT; Not treated, IPA; Isopropyl alcohol, RT; Room temperature, HT; High temperature.

4. SEM surface morphology

Figure 10A show the SEM images of different post-processed specifications at $100\times$ magnifications with region of interest in labial gingival third. The IPA group showed the most uneven surface, but it appeared to have a consistent pattern (Figure 10B). No layer was observed in the NT (Figure 10C) and RT-2 mins group, and the NT group showed the smoothest surface. SEM images of RT-4, 6 mins (Figure 10D) and HT-2, 4, 6 mins (Figure 10E) groups showed similar surface morphology, and the printed layer could clearly be observed. Among them, the printed layer of the specimen of the HT-6 mins group was most clearly observed. These results may be related to the results of measuring the weight of the clear aligner. It can be inferred that the more clearly the layer is visible on the transparent clear aligner surface, the less monomer remains.

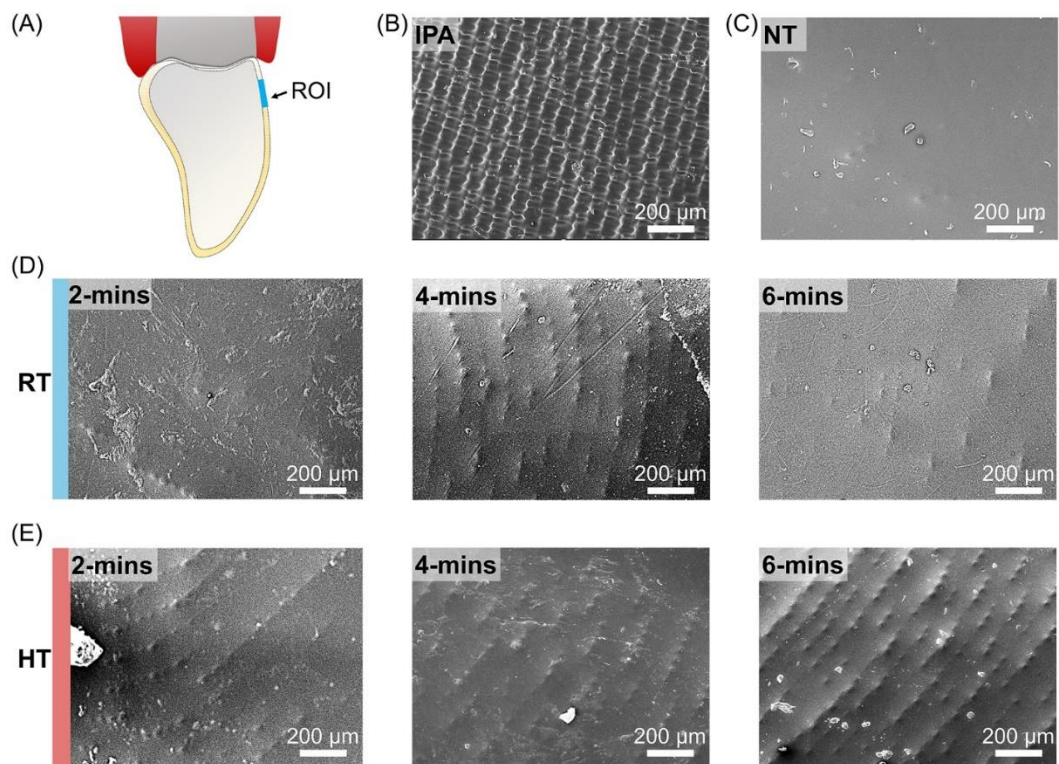


Figure 10. SEM image ($\times 100$ magnification) of clear aligners: (A) A schematic diagram of the SEM image capture locations, (B) IPA, (C) NT, (D) RT-2, 4, 6 and (E) HT-2, 4, 6. NT; Not treated, IPA; Isopropyl alcohol, RT; Room temperature, HT; High temperature.

5. Relative assessment of clear aligner geometry

This study used a color-difference map to qualitatively compare the effect of inadequate uncured monomer removal on fit of clear aligner (Figure 11A). The index of the color-difference map was set to $\pm 100 \mu\text{m}$, and the differences between the two groups were expressed as color differences. Positive (+) deviations are shown in red, the closer the deviation is to 0, the more the color is green, and negative (-) deviations are shown in blue. As a result, the distribution of color-difference maps was similar aside from the NT group. In the NT group, positive deviations were prominent with a large red areas appearing in the anterior incisal region (Figure 11B), while no red areas were observed at all in the other groups. RT-2 mins were within the tolerance range (green color). Yellow color appeared on the lingual part of the canine tooth in the RT and HT groups, aside from RT-2 mins (Figure 11C, D). In terms of RMS value, the NT group had a significantly larger RMS value ($p < 0.05$) compared to the other groups, while there was no significant difference in the RMS value of the other groups (Table 2).

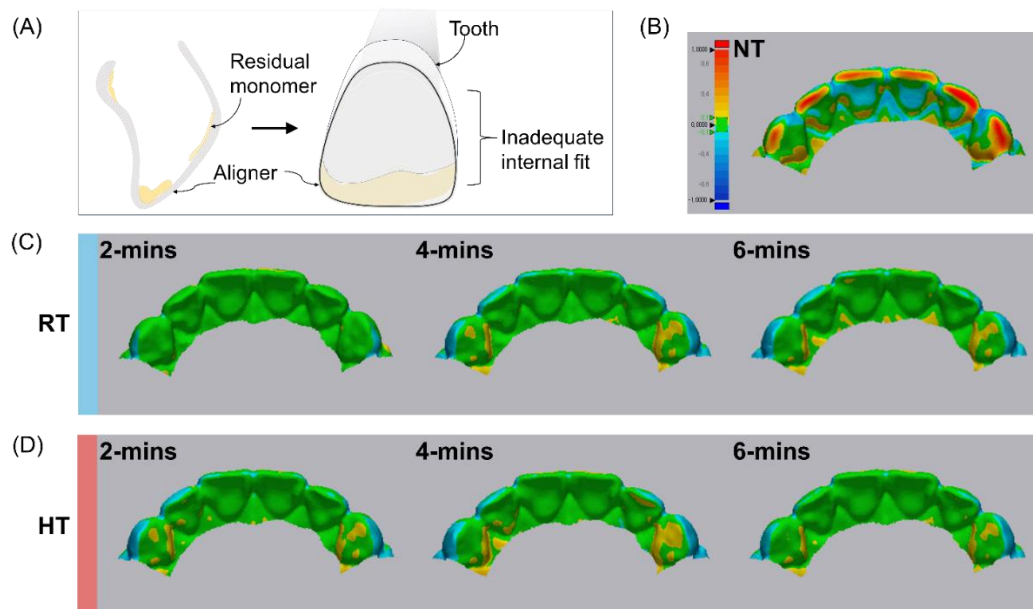


Figure 11. Comparison of color difference maps of anterior region evaluated by using Geomagic software program: (A) A schematic diagram illustrating the residual monomer pattern on the printed clear aligner before the cleaning process; (B) NT; (C) RT-2, 4, 6; (D) HT-2, 4, 6. NT; Not treated, RT; Room temperature, HT; High temperature.

Table 3. The accuracy of seven groups for anterior expressed in root mean square with SD (μm)

Group	NT	RT-2	RT-4	RT-6	HT-2	HT-4	HT-6
Mean	0.38 ^a	0.16 ^b	0.14 ^b	0.20 ^b	0.19 ^b	0.16 ^b	0.17 ^b
\pm SD	0.04	0.01	0.01	0.02	0.03	0.01	0.02

Different lowercase letters indicate significant differences in the average between groups ($p < 0.05$). NT; Not treated, RT; Room temperature, HT; High temperature.

6. Results of stress relaxation

All groups showed an increasing trend in the shape recovery ratio over time (Table 4). Upon 60 mins of relaxation all groups exhibited a shape recovery rate of over 95 %. Results revealed a significant main effect of shape recovery time ($p < 0.05$). However, no significant main effect was observed between treatment groups ($p > 0.05$). This suggests that the pattern of shape recovery ratio change over time was similar across all treatment groups. Although not statistically significant, a trend was observed where HT groups showed slightly higher shape recovery ratios compared to RT groups at the 30-minute and 60-minute time points.

Table 4. Shape recovery ratio of clear aligners specimens (%)

Time (mins)	NT	RT-2	RT-4	RT-6	HT-2	HT-4	HT-6
0	48.29 ± 2.98 ^{Aa}	45.86 ± 1.32 ^{Aa}	44.28 ± 2.69 ^{Aa}	44.00 ± 2.72 ^{Aa}	46.44 ± 2.90 ^{Aa}	48.26 ± 2.11 ^{Aa}	46.81 ± 1.87 ^{Aa}
10	79.74 ± 5.66 ^{Ab}	81.60 ± 9.33 ^{Ab}	75.64 ± 9.91 ^{Ab}	83.44 ± 5.41 ^{Ab}	79.10 ± 9.73 ^{Ab}	80.32 ± 8.91 ^{Ab}	74.88 ± 3.61 ^{Ab}
30	92.18 ± 2.49 ^{Ac}	90.82 ± 4.26 ^{Ac}	91.74 ± 3.73 ^{Ac}	93.35 ± 3.73 ^{Ac}	95.32 ± 1.87 ^{Ac}	94.91 ± 5.11 ^{Ac}	92.91 ± 3.09 ^{Ac}
60	96.80 ± 1.01 ^{Ad}	96.93 ± 2.94 ^{Ad}	95.91 ± 1.21 ^{Ad}	98.79 ± 1.77 ^{Ad}	99.23 ± 1.16 ^{Ad}	99.37 ± 3.82 ^{Ad}	98.70 ± 4.17 ^{Ad}

Same capital letters indicate no significant differences in the average between groups at the same time points ($p > 0.05$). Different lowercase letters indicate significant difference between relaxation time within the same group ($p < 0.05$). NT; Not treated, RT; Room temperature, HT; High temperature.

7. Cytotoxicity analysis

Figure 12 presents the cell viability data for various tested groups. The cell viability values are as follows: 98.99 ± 8.78 % for the negative control, 8.35 ± 0.20 % for the positive control, 82.1 ± 4.46 % for the NT group, 92.98 ± 1.64 % for the IPA group, and for the RT-2, RT-4, and RT-6 groups, the values are 89.31 ± 3.61 %, 87.90 ± 6.80 %, and 97.26 ± 2.06 % respectively. The HT-2, HT-4, and HT-6 groups have cell viability values of 84.88 ± 9.04 %, 91.02 ± 8.90 %, and 87.61 ± 2.77 % respectively. Notably, the IPA, RT-6 and HT-4 groups exhibited significantly higher cell viability in comparison to the other experimental groups ($p < 0.05$).

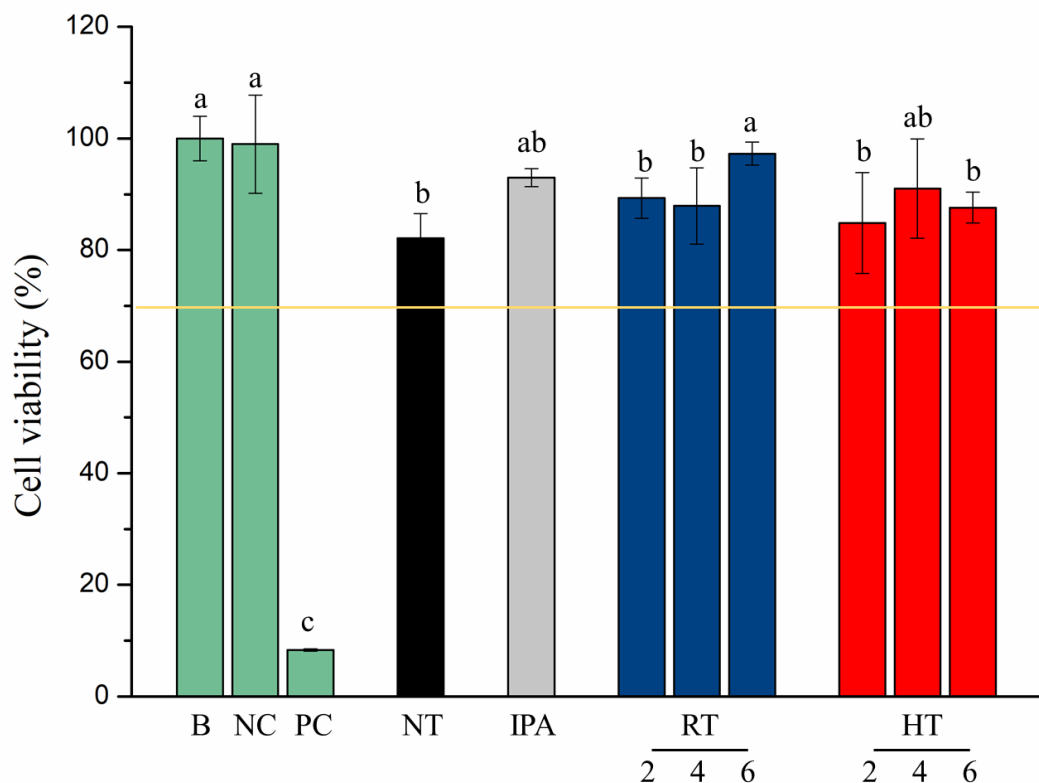


Figure 12. Cell viability of clear aligner model for each experimental group compared to the blank (B). The yellow line represents the minimum ISO standard (ISO 10993-5, 2009) criterion: a cell viability less than 70 % is considered cytotoxic. When lowercase letters above the bar graph are the same, it signifies that there are no significant differences between the groups ($p < 0.05$). Conversely, differing lowercase letters indicate significant differences between the groups ($p < 0.05$). B; blank, NC; negative control, PC; positive control, NT; Not treated, IPA; Isopropyl alcohol, RT; Room temperature, HT; High temperature.

IV. DISCUSSION

The present study investigated the time and temperature of a centrifugation cleaning method for the removal of uncured monomer fraction from 3D-printed clear aligners, while focusing on their surface characteristics and optical features. The results demonstrated that, while increases in time and temperature did not alter the surface properties, it affected translucency and the internal surface morphology of aligners.

Recent advancements in clear aligner production have leveraged additive manufacturing due to its high precision and ease of production. Given the importance of aligners' physical and optical qualities, an organic-solvent-free centrifugation method has been suggested as a method that could be used for effective removal of any uncured monomer. Although a basic centrifugation protocol is established, knowledge of the most effective settings primarily relies on empirical evidence. To explore the optimal physical conditions for effective centrifugation, the centrifuge equipment was modified to operate at a standard RPM, and a heating element was added around the chamber's edge. It was carefully verified that the heating element did not come into contact with the rotating chamber to maintain rotational efficiency (Figure 4). Temperature control was achieved through a digital thermostat, and cycle durations were adjusted manually. Moreover, for efficient centrifugation, clear aligners were loaded in a balanced way in each cycle.

To characterize the fundamental response of the provided resin to heat, experiments were conducted to observe its viscosity and flow properties. The resin exhibited a predictable increase in flow when heated, which was consistent with viscosity profiles that are typical of most liquid-type resins at elevated temperatures (Jamal et al., 2020). There is also a direct correlation between the viscosity of a liquid and its flow rate. In a solvent-free centrifuge setup, this relationship could play a crucial role in effectively removing the uncured monomer fraction (Gandhi et al., 2022). In this study, the 3D-printing resin demonstrated approximately a 2.34-fold increase in flow upon heating to 55 °C, which ultimately resulted in increased flowability and decreased viscosity. When evaluating the

viscosity change under both temperature and physical shear force, the clear aligner resin exhibited a significant reduction in viscosity, approaching zero Pascal-seconds. This finding further supports the idea that centrifugal cleaning effectiveness can be enhanced by increasing the chamber temperature.

Transparency in clear aligner is the key to the aligner's clinical compliance and treatment success (Cremonini et al., 2022). The optical properties of materials are determined by how they respond to light in terms of absorbance and transmittance. The higher the transmittance of material, the more transparent it is; conversely, higher the absorbance, the less transparent the material (Watts and Cash, 1994). In the case of a transparent non-scattering medium, the transmittance is inversely proportional to the thickness of the sample according to the Beer-Lambert law ($T = \exp(-\mu_a d)$, where T is the transmittance, d is the sample thickness, and μ_a is the absorption coefficient) (Chen et al., 2019). In a previous study, Clear aligner produced using IPA and centrifuge washing methods was measured to be thinner in the IPA washing group. However, the transparency of the IPA washed group was shown to be significantly reduced (Park et al., 2023).

Previous research has also demonstrated that, beyond the rinsing solution, the time and method also significantly affect the surface morphology and roughness of materials (Lambart et al., 2022; Mayer et al., 2021). The findings of the present study also add to this evidence corroborating that chemical and non-chemical cleaning techniques differently affect the surfaces of 3D-printed clear aligners. Analyzing the SEM images alongside transmittance data, it could be observed that the IPA group, which displayed the lowest levels of light transmittance, had the most irregular surface texture. Conversely, the NT group surface was considerably smoother compared to those of the other groups.

The findings of our study are consistent with these observations. Moreover, SEM revealed noticeable differences in the inner surface of the clear aligners with increasing temperature. These outcomes suggest that the removal of uncured monomer reveals the micro-surface fingerprints characteristic of 3D printing (Li et al., 2023). Such exposure

could indirectly affect light transmission and in turn affect the translucency of the clear aligners, regardless of their thickness. Furthermore, while no significant changes were observed in the weight of the aligners, variations in translucency were noted with changes in temperature.

In the group where layering was evident in the SEM images, the inter-layer spacing appeared to exceed 50 μm , diverging from the predefined layer thickness settings during the printing process. This discrepancy arises because the specimens in this study were not produced as flat shapes but rather as 3D-printed clear aligners. Further, clear aligners printed at 45 degrees have intermediate options between horizontal and vertical orientations in terms of print layers, print time, and space taken up on the build platform, so these parts are printed at an oblique angle (McCarty et al., 2020). The choice to photograph the cervical third of the aligner was deliberate, as this area is most distinct and offers a high contrast between the gum tissue and tooth; this is particularly noticeable when people smile or talk (Kobayashi et al., 2021; Wang et al., 2013). Enhancing the printing resolution, specifically the layer proximity, might mitigate this effect, which is a relationship that might requires further research.

The accuracy of clear aligner adaptation was assessed by comparing the internal surface morphology to the intended design. The quality of the aligner's fit on the tooth surface significantly influences the effectiveness of orthodontic tooth movement (McCarty et al., 2020; Weir, 2017). Given that clear aligners cover all exposed anatomical surfaces of a tooth, any misalignment can substantially disrupt the intended tooth movement. Misalignments could also result in premature occlusal interference, ultimately leading to discomfort and potential adverse effects (Castroflorio et al., 2023).

Considering the poor translucency, the IPA group was excluded from the internal fit assessment. The differences among the centrifugation groups were qualitatively evaluated using color map analysis. In this analysis, a yellow-red gradient indicates an area where the clear aligner thickness has increased non-uniformly internally, due to aggregation of

uncured monomer post-centrifugation. Meanwhile, a cyan to blue gradient an area where the surface has become thinner. To provide a baseline for comparison, a morphometric analysis of the NT group was performed. As seen in the 3D-color map difference analysis in Figure 11A inefficient resin removal adversely affects the incisor edge which is a geometrically tapered region. A clear aligner experiencing this issue is likely to fails in properly engage the tooth surface, which can lead to an unintentional increase in the incisal dimension or complete loss of fit. This, in turn, may cause severe discomfort.

The centrifugation groups did not exhibit statistically significant differences in RMS values with variations in time and temperature. However, qualitative assessments revealed well-aligned incisal edges for both HT and RT conditions at 2 minutes. Further, the adaptation at the cingulum surface on the palatal side towards the mesial line angle of the canine showed a sporadic yellow gradient. This indicates that the arch's curvature might affect the efficiency of removing uncured monomer following 3D printing. A previous study that compared internal fit also identified a potential gap near the cingulum surface in the gingival third of the anterior region (Park et al., 2023). Although they used micro-computed tomography for their assessment, their findings are consistent with those of the current study. Moreover, the RMS value was derived by creating a 3D model from the internal surface of the clear aligner, essentially using it as a mold. Given the indirect nature of this assessment method, objectively generalizing the RMS results presents a challenge. In addition, the absence of a definitive, practical guideline for evaluating clear aligner fit complicates the achievement of a high-precision methodology. Despite these challenges, the methodology employed is detailed in such a manner that supports reproducibility in future research.

The arch-width at the intermolar region is a dynamic value that changes significantly with an individual's development. In orthodontic treatment, avoiding any unwarranted reduction in IM is crucial for outcome stability. By analyzing the stress relaxation-driven shape recovery, it was confirmed that there was no unwarranted reduction in width, with over 95 % recovery observed after 60 minutes. This finding is consistent with previous

studies that demonstrated an increase in recovery rate over time during bending tests. This suggests that the centrifugation cleaning time and temperature do not significantly compromise the shape memory properties of clear aligners, which are crucial for their clinical performance and treatment outcomes (Lee et al., 2022).

Lastly, 3D-printing resins are highly cytotoxic prior to the 3D-printing process, and cytotoxic levels are significantly reduced after post-polymerization procedures to remove uncured monomer (Oh et al., 2023). In this study, there was a statistically significant difference in the cell viability values between experimental groups; however, there was no trend which increasing time or temperature. The NT group showed the lowest cell survival rate among the experimental groups. All groups were found to comply with ISO 10993-5 standards. This suggests that it is biocompatible for oral use regardless of cleaning method.

Despite the comprehensive findings, this study has several limitations. First, it is due to the fact that there are currently no standardized indicators or standards that can define the transparency of clear aligners. Therefore, this study had no choice but to conduct only a relative evaluation, not an absolute evaluation, of the transparency of clear aligners.

In addition, in this study, a clear aligner produced by scanning a standardized typodont model was used. In actual clinical practice, clear aligners are used on patients with various abnormal dentitions. Therefore, further research is needed to determine whether the same cleaning method would yield the same effects when applied to clear aligners for patients with severe crowding.

Lastly, the study was conducted using one type of cleaning machine and fixed centrifugal force (27.95 g), but additional research is needed to investigate how different centrifugal forces affect the cleaning efficiency and material properties of the 3D printed clear aligner.

This study has implications beyond orthodontic clear aligners. Recently, the centrifugal cleaning method has been used in dentistry to produce temporary 3D-printed fixed dental

prostheses. Research that conducted centrifugal cleaning using various 3D printing materials have shown that, unlike mechanical cleaning, chemical cleaning impairs flexural strength, and the cleaning strategy recommended by individual manufacturers does not always result in the highest mechanical properties for each material (Mayer et al., 2021). Although our study primarily focused on clear aligners, the results can have a wide-ranging impact across dental restorative treatments. It is hoped that the findings of this study will contribute to the advancement of dental 3D-printing technology and the expansion of its clinical applications.

V. CONCLUSION

The current study aimed to investigate the optimal centrifugation cleaning time and temperature conditions in the post-processing cleaning stage of 3D printing to effectively remove uncured monomers while preserving the (i) weight, (ii) optical transparency, (iii) internal surface morphology, (iv) stress relaxation and (v) cytotoxicity of clear aligners.

The key findings of this research were as follows:

- (1) The centrifugation cleaning method significantly affected the weight of the clear aligners, with higher temperatures and longer durations resulting in greater weight reduction. This suggests that the uncured monomer removal was more effective under these conditions.
- (2) The IPA group showed the lowest transmittance values, which had detrimental effect on optical clarity. However, there were no significant differences in the transparency of the RT-2, 4, 6, and HT-2, 4, 6 groups according to centrifugation time and temperature.
- (3) The internal surface morphology of the clear aligners was evaluated using a color-difference map. The distribution of color-difference maps was similar among the centrifugation groups, but the NT group showed prominent positive deviations in the anterior incisal region. The RMS value of the NT group was significantly larger than that of the other groups, while there were no substantial differences among the centrifugation groups.
- (4) The shape recovery ratio due to stress relaxation recovered more than 95 % for the IM after 60 minutes in all group, and there were no significant differences in the shape recovery ratio based on time and temperature.

(5) Cytotoxicity analysis results showed that all groups met the ISO standard requirements, but there were significant differences between the groups.

The first and fifth null hypotheses were rejected, while the second, third, and fourth null hypotheses were accepted.

Considering these findings, it can be concluded that centrifugal cleaning at a high temperature of HT for 2 minutes using a centrifuge with a force of 27.95 g is expected to provide the same cleaning effect as the manufacturer's recommended 6-minute cleaning process. This optimized cleaning protocol may lead to shorter working times in clinical settings while maintaining the desired properties of the clear aligners.

REFERENCES

- Bichu YM, Alwafi A, Liu X, Andrews J, Ludwig B, Bichu AY, et al.: Advances in orthodontic clear aligner materials. *Bioactive Materials* 22:384-403, 2023.
- Bowers LN, Stefaniak AB, Knepp AK, LeBouf RF, Martin Jr SB, Ranpara AC, et al.: Potential for Exposure to Particles and Gases throughout Vat Photopolymerization Additive Manufacturing Processes. *Buildings* 12(8):1222, 2022.
- Caelli C, Tamburrino F, Brondi C, Razonale AV, Ballarino A, Barone S: Sustainability in Healthcare Sector: The Dental Aligners Case. *Sustainability* 15(24):16757, 2023.
- Castroflorio T, Sedran A, Parrini S, Garino F, Reverdito M, Capuozzo R, et al.: Predictability of orthodontic tooth movement with aligners: effect of treatment design. *Progress in Orthodontics* 24(1):2, 2023.
- Chen H, Baitenov A, Li Y, Vasileva E, Popov S, Sychugov I, et al.: Thickness Dependence of Optical Transmittance of Transparent Wood: Chemical Modification Effects. *ACS Applied Materials & Interfaces* 11(38):35451-35457, 2019.
- Cremonini F, Vianello M, Bianchi A, Lombardo L: A Spectrophotometry Evaluation of Clear Aligners Transparency: Comparison of 3D-Printers and Thermoforming Disks in Different Combinations. *Applied Sciences* 12(23):11964, 2022.
- Dong X: Analysis of Factors Affecting the Dehydration Effect of Centrifugal Dehydrator. In: *2020 7th International Forum on Electrical Engineering and Automation (IFEEA)*. IEEE, 2020. p. 178-181.
- Gandhi K, Sharma N, Gautam PB, Sharma R, Mann B, Pandey V: Centrifugation. In: *Advanced Analytical Techniques in Dairy Chemistry*. Springer, 2022. p. 85-102.
- Grant J, Foley P, Bankhead B, Miranda G, Adel SM, Kim KB: Forces and moments generated by 3D direct printed clear aligners of varying labial and lingual thicknesses during lingual movement of maxillary central incisor: an in vitro study. *Progress in Orthodontics* 24(1):23, 2023.
- ISO 10993-5:2009. Biological evaluation of medical devices - Part 5: Tests for in vitro cytotoxicity. *International Organization for Standardization, Geneva*, 2009.
- ISO 10993-12:2012. Biological evaluation of medical devices - Part 12: Sample preparation and reference materials. *International Organization for Standardization, Geneva*, 2012.
- Jamal DN, Shajahan MM, Abhineshjayram M, Goutham S: Empirical investigation and comparison of different viscosity liquids with increasing temperature. In: *2020 International Conference on Emerging Trends in Information Technology and Engineering (ic-ETITE)*. IEEE, 2020. p. 1-4.
- Jang W, Kook G-S, Kang J-H, Kim Y, Yun Y, Lee S-K, et al.: Effect of washing condition on the

fracture strength, and the degree of conversion of 3D printing resin. *Applied Sciences* 11(24):11676, 2021.

Kesling HD: The philosophy of the tooth positioning appliance. *American Journal of Orthodontics and Oral Surgery* 31(6):297-304, 1945.

Kobayashi S, Nakajima M, Furusawa K, Tichy A, Hosaka K, Tagami J: Color adjustment potential of single-shade resin composite to various-shade human teeth: Effect of structural color phenomenon. *Dental Materials Journal* 40(4):1033-1040, 2021.

Koenig N, Choi J-Y, McCray J, Hayes A, Schneider P, Kim KB: Comparison of dimensional accuracy between direct-printed and thermoformed aligners. *Korean Journal of Orthodontics* 52(4):249-257, 2022.

Lambart A-L, Xepapadeas AB, Koos B, Li P, Spintzyk S: Rinsing postprocessing procedure of a 3D-printed orthodontic appliance material: Impact of alternative post-rinsing solutions on the roughness, flexural strength and cytotoxicity. *Dental Materials* 38(8):1344-1353, 2022.

Lee SY, Kim H, Kim H-J, Chung CJ, Choi YJ, Kim S-J, et al.: Thermo-mechanical properties of 3D printed photocurable shape memory resin for clear aligners. *Scientific Reports* 12(1):6246, 2022.

Li H, Liang L, Deng Y, Ge N, Shan W: 3D printing polyurethane acrylate (PUA) based elastomer and its mechanical behavior. *Materials Research Express*, 2023.

Mayer J, Reymus M, Mayinger F, Edelhoff D, Hickel R, Stawarczyk B: Temporary 3D-Printed Fixed Dental Prosthesis Materials: Impact of Postprinting Cleaning Methods on Degree of Conversion and Surface and Mechanical Properties. *International Journal of Prosthodontics* 34(6), 2021.

McCarty MC, Chen SJ, English JD, Kasper F: Effect of print orientation and duration of ultraviolet curing on the dimensional accuracy of a 3-dimensionally printed orthodontic clear aligner design. *American Journal of Orthodontics and Dentofacial Orthopedics* 158(6):889-897, 2020.

Oh R, Lim J-H, Lee C-G, Lee K-W, Kim S-Y, Kim J-E: Effects of washing solution temperature on the biocompatibility and mechanical properties of 3D-Printed dental resin material. *Journal of the Mechanical Behavior of Biomedical Materials* 143:105906, 2023.

Park SY, Choi S-H, Yu H-S, Kim S-J, Kim H, Kim KB, et al.: Comparison of translucency, thickness, and gap width of thermoformed and 3D-printed clear aligners using micro-CT and spectrophotometer. *Scientific Reports* 13(1):10921, 2023.

Rajasekaran A, Chaudhari PK: Integrated manufacturing of direct 3D-printed clear aligners. *Frontiers in Dental Medicine* 3:1089627, 2023.

Reymus M, Fabritius R, Keßler A, Hickel R, Edelhoff D, Stawarczyk B: Fracture load of 3D-printed fixed dental prostheses compared with milled and conventionally fabricated ones: the impact of resin material, build direction, post-curing, and artificial aging—an in vitro study. *Clinical Oral Investigations* 24:701-710, 2020.

Ryan T, Hubbard D: 3-D printing hazards: Literature review & preliminary hazard assessment. *Professional Safety* 61(06):56-62, 2016.

Vasamsetty P, Pss T, Kukkala D, Singamshetty M, Gajula S: 3D printing in dentistry–Exploring the new horizons. *Materials Today: Proceedings* 26:838-841, 2020.

Wang J, Lin J, Seliger A, Gil M, da Silva JD, Ishhikawa-Nagai S: Color effects of gingiva on cervical regions of all-ceramic crowns. *Journal of Esthetic and Restorative Dentistry* 25(4):254-262, 2013.

Watts DC, Cash AJ: Analysis of optical transmission by 400–500 nm visible light into aesthetic dental biomaterials. *Journal of Dentistry* 22(2):112-117, 1994.

Weir T: Clear aligners in orthodontic treatment. *Australian Dental Journal* 62:58-62, 2017.

Youm J-H, Jeong IJ, Kwon J-S, Lim B-S, Oh M-H, Kim K-M: The optical property measuring methods for resin composite using multiple spectrophotometers. *Dental Materials Journal*:2023-2312, 2024.

ABSTRACT (IN KOREAN)

3D 프린팅 후처리 과정에서 원심분리 시간 및 온도에 따른

투명 교정 장치 미경화 단량체 제거 효율

<지도교수 권 재 성>

연세대학교 대학원 치의학과

김 지 은

3D 프린팅 기술의 발전으로 치과용 CAD 설계로부터 투명한 레진 재료를 사용하여 직접 맞춤형 투명 교정 장치의 제작이 가능해졌다. 이러한 3D 프린팅 투명 교정 장치를 제작하기 위해서는 환자의 치열을 3D 스캔하고, 각 교정 단계별 목표 모델을 설계한 뒤 프린터로 인쇄한다. 인쇄가 완료된 투명 교정 장치는 플랫폼에서 분리되어 일련의 후처리 과정을 거치게 되는데, 이 중 미경화 단량체를 제거하는 세척 단계는 정확한 교정 장치의 제작과 적절한 물성을 확보하는데 있어 매우 중요하다.

기존에 이소프로필 알코올(이하 IPA)을 사용한 화학적 세척법의 단점이 대두되며 최근 비화학적 세척법인 원심분리 세척법이 주목받고 있다. 본 연구에서는 3D 프린팅 투명 교정 장치에서 미경화 단량체를 제거하는 데 있어 원

심분리 세척방법의 온도와 시간이 미치는 영향을 조사하였다.

세척 온도 환경은 원심분리기 안쪽에 설치한 열선을 통해 제어되었다. 3D 프린팅 투명 교정 장치를 IPA 또는 각각 $23 \pm 2^\circ\text{C}$ (이하 RT) 와 $55 \pm 2^\circ\text{C}$ (이하 HT)에서 2, 4, 6분 동안 원심분리(중력가속도 27.95 g)로 세척한 후 유동학, 무게 측정, 투명도 평가, 표면 분석, 3D 데이터 비교, 응력 이완 특성 및 세포독성 평가를 수행하였다.

그 결과, HT 에서 RT 보다 점도가 2.34배 감소하였고, 원심분리 세척 온도와 시간이 증가할수록 투명 교정 장치의 무게가 감소하는 것으로 나타났다($p < 0.05$). 투명도를 결정하기 위해 자외선 가시 분광 광도계로 측정한 투과도 값은 IPA 그룹에서 가장 낮았고, 온도와 시간이 증가할수록 투과도 값이 낮아지는 경향을 보였다. IPA 그룹은 다른 그룹들과 유의하게 낮은 투명도를 보였다($p < 0.05$). 투명 교정 장치 시편의 투명도를 육안으로 관찰하였을 때는 IPA 그룹을 제외한 나머지 그룹은 차이가 없었다. 주사전자현미경으로 표면을 관찰한 결과 IPA 그룹의 표면이 가장 거칠게 관찰되었다. 투명 교정 장치의 내부 적합도를 측정하고자 제작한 석고 모델의 3D 스캔을 통한내면 적합도 평가 결과, 원심분리 세척을 진행한 그룹은 비교적 우수한 정밀도를 나타냈다. 세척하지 않은 그룹은 Root Mean Square값이 높았을 뿐만 아니라($p < 0.05$) 절단 부위가 붉게 나타나 양(+)의 편차를 보였다. 형상 기억 특성을 확인하기 위해 수행한 응력 이완 시험 결과, 시간이 지남에 따라 교정 장치의 형태가 회복되었으며, 60 분 경과 후에는 모든 그룹이 95 % 이상 회복률을 보였고, 세척 방법에 따른 유의한 차이는 없었다($p > 0.05$). 실험 그룹간 세포독성은 유의한 차이가 없었고, 모든 값이 ISO에 따른 세포독성 평가 기준을 충족하였다.

이상의 결과를 종합해 볼 때, 온도와 시간에 따른 미경화 단량체 제거 효

을 및 일부 물성에는 유의한 차이가 나타났으나, 세포독성과 응력 이완 거동에는 큰 영향이 없었다. 특히, HT에서 2분간 원심분리 세척을 적용하였을 때 미경화 단량체가 효과적으로 제거하면서도 장치의 물리적 특성 (무게, 투명도, 표면 특성, 치수 안정성 및 형상 회복률)이 잘 유지되었다. 따라서 HT에서 2분간 원심분리를 진행하는 것이 작업시간을 최소화하며, 미경화 단량체를 효과적으로 제거하면서도 투명 교정 장치의 물리적 특성에 큰 영향을 미치지 않아 적절한 임상적 세척 방법이라고 사료된다.

핵심되는 말: 원심분리, 투명 교정 장치, 3D 프린팅, 후처리, 원심분리 세척, 시간, 온도